



Characterization of Blasted Austenitic Stainless Steel and Its Corrosion Resistance

F. Otsubo, K. Kishitake, T. Akiyama, and T. Terasaki

(Submitted 4 September 2002; in revised form 11 November 2002)

It is known that the corrosion resistance of stainless steel is deteriorated by blasting, but the reason for this deterioration is not clear. A blasted austenitic stainless steel plate (JIS-SUS304) has been characterized with comparison to the scraped and non-blasted specimens. The surface roughness of the blasted specimen is larger than that of materials finished with #180 paper. A martensite phase is formed in the surface layer of both blasted and scraped specimens. Compressive residual stress is generated in the blasted specimen and the maximum residual stress is formed at 50-100 μm from the surface. The corrosion potentials of the blasted specimen and subsequently solution treated specimen are lower than that of the non-blasted specimen. The passivation current densities of the blasted specimens are higher than those of the non-blasted specimen. The blasted specimen and the subsequently solution treated specimen exhibit rust in 5% sodium chloride (NaCl) solution, while the non-blasted specimen and ground specimen do not rust in the solution. It is concluded that the deterioration of corrosion resistance of austenitic stainless steel through blasting is caused by the roughed morphology of the surface.

Keywords austenitic stainless steel, blasting, corrosion resistance, martensite phase, residual stress, surface roughness

1. Introduction

Ceramic coatings by plasma spraying onto metallic materials are applied to provide wear resistance, corrosion resistance and heat protection in many industrial fields. Ceramic coatings themselves exhibit excellent intrinsic corrosion resistance but sealing of pores is usually needed to prevent solution reaching to the metallic substrate. Process rolls made of austenitic stainless steel (JIS-SUS304^[1]) with plasma-sprayed alumina coating are used in the paper making industry. Stains might appear on the alumina surface if the sealing operation is not perfect, even if the rolls are used under conditions where the SUS304 steel does not rust. It is expected that stains on the alumina surface are caused by deterioration of the stainless steel through the grit blasting process prior to plasma spraying.

Figure 1 shows a SUS304 steel plate grit-blasted with alumina after a salt spray test for 250 h.^[2] It is observed that the blasted surface of SUS304 steel rusts after the test, although non-blasted SUS304 steel does not rust under the same conditions. Figure 2 shows the alumina coating plasma sprayed on the blasted SUS304 steel substrate without a sealing process and the specimen after corrosion test in 5% sodium chloride (NaCl) solution. It is confirmed that the rust appears on the surface of the coating from SUS304 steel substrate through pores.

Since the blasting process forms plastic deformation on the substrate surface, residual stress may develop in the blasted surface layer. Microstructural features such as lattice defects may influence the corrosion resistance of stainless steels.^[3,4] Further-

more, it is reported that the natural corrosion potential depends on the surface roughness.^[5] Accordingly, it is considered that the blasting process affects the corrosion behavior of SUS304 steel.

There are few reports concerning the effect of blasting on the corrosion resistance of SUS304 steel.^[6] For the present work, the characterization of surface condition, structure, and residual stress distribution, as well as corrosion resistance of SUS304 steel plates blasted with alumina grits were been investigated. Factors affecting the corrosion resistance were examined by electrochemical and corrosion tests.

2. Experimental Procedure

A commercial austenitic stainless steel plate of JIS-SUS304 was solution treated at 1273 K to remove the effect of prior cold rolling. The surface layer was abraded by about 0.2 mm from the surface with #400 abrasive paper in wet and then finished by buffing with 0.05 μm alumina powder before roughening. Since the inherent strain is not developed by grounding with #400 abrasive paper,^[7] the polishing process with #400 abrasive paper does not generate residual stress in the specimen. The blasting was performed so that specimens were uniformly roughened using an air blast machine under the conditions shown in Table 1. The specimen ground with #180 abrasive paper under dry conditions and the specimen polished electrolytically after polishing with #400 abrasive paper to remove the layer having a martensite phase were also prepared for comparison. Grinding with abrasive paper was performed under standard conditions of 400 cycles under 29.4 N load using a Suga abrasive tester (NUS-ISO3 Suga Test Instruments Co., Ltd., Tokyo, Japan).^[8]

Surface roughness of the specimens was measured using a roughness tester (SURF TEST 301 Mitutoyo Corporation, Kawasaki, Japan). The structure of the surface layer of the specimen was examined by x-ray diffraction (XRD). The residual stress distribution through the thickness was measured by the inherent strain method.^[9] The corrosion resistance of the speci-

F. Otsubo, K. Kishitake, T. Akiyama, and T. Terasaki, Department of Materials Science and Engineering, Faculty of Engineering, Kyushu Institute of Technology, 1-1 Sensui Tobata Kita-Kyushu 804-8550, Japan. Contact e-mail: otsubo@tobata.isc.kyutech.ac.jp.

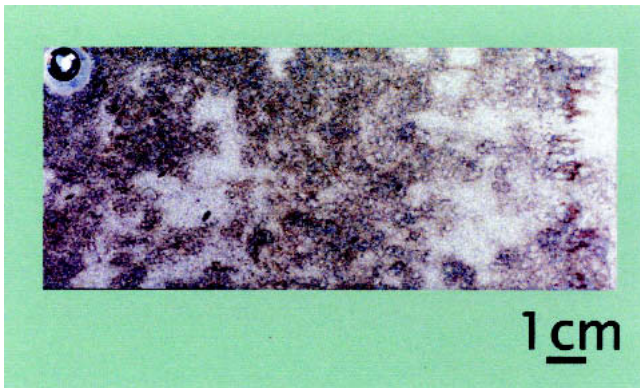


Fig. 1 Grit-blasted austenitic stainless steel plate after a 250h salt spray test

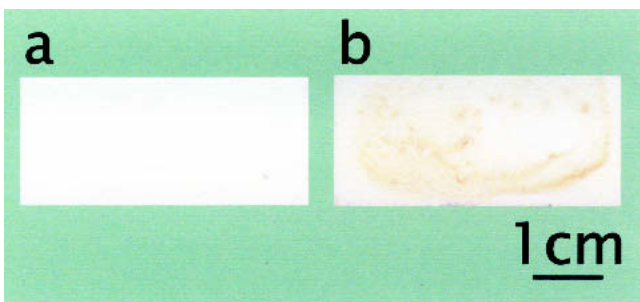


Fig. 2 Alumina coating surface on SUS304 substrate: (a) as-sprayed, (b) after immersion test

Table 1 Blasting Condition

Blasting media	# 24 Alumina grit
Air pressure	0.6 MPa
Angle	75°
Nozzle opening	8 mm (in diameter)
Work distance	100 mm
Blasting time	60 s

mens was evaluated from anodic polarization curves measured using a potentiostat in de-aerated 1 N H_2SO_4 solution at 303 K and a corrosion test in 5% NaCl solution. The opposite electrode and reference electrode used were platinum and saturated calomel for the measurement of anodic polarization curves, respectively. The surface of specimen was masked with acid-resistant lacquer to expose an area of 100 mm^2 for the measurement. The measurement was carried out by scanning the corrosion potential to +1.1 V (versus SCE) with a scanning rate of 60 mV min^{-1} after holding at -0.7V(versus SCE) for 0.6 ks. A water-line attack test at room temperature was applied for the corrosion test in 5% salt water.

3. Results and Discussion

3.1 Surface Roughness

Figure 3 shows profiles of the surface roughness of specimens roughened by grit blasting and grinding with #180 abrasive paper. The roughness of the blasted specimen is large com-

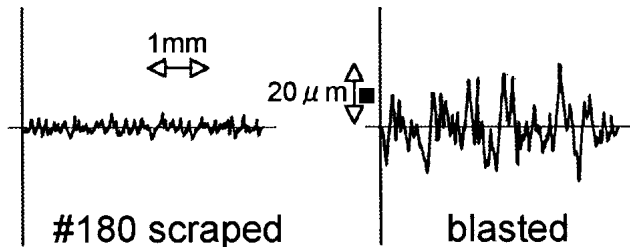


Fig. 3 Surface roughness profiles of specimens

pared with the specimen ground with #180 abrasive paper. An average roughness value (R_a) of the specimen ground with #180 abrasive paper was $0.87 \mu\text{m}$ while that of the grit-blasted specimen was about seven times larger.

3.2 Structure of Blasted Specimen

Figure 4 shows XRD patterns of the surface of the roughened specimens. Diffraction peaks of the solution treated specimen are of only austenite phase. A large diffraction peak of martensite phase appears in the XRD pattern of the specimen ground with #180 abrasive paper. The diffraction peak of martensite phase is also seen for the blasted specimen but it is smaller compared with the specimen ground with #180 abrasive paper. This implies that the volume fraction of martensite phase on the surface layer of the grit-blasted specimen is smaller than that of the ground specimen. Martensite phase may be formed by plastic deformation^[10,11] through roughening and martensite in austenite phase might deteriorate the corrosion resistance.^[12]

The diffraction peak of martensite phase disappears in the XRD pattern of the ground specimen after electrolytic polishing and removing several micrometers material. Figure 5 shows the XRD patterns of the grit-blasted surface and subsequent surfaces obtained by removing surface layers by electrolytic polishing to $150 \mu\text{m}$ in depth. The peak of the martensite phase shows a maximum at a depth of around $25 \mu\text{m}$ from the surface and almost disappears at $100 \mu\text{m}$. It is understood that martensite phase forms in the surface layer to a depth of about $100 \mu\text{m}$ from the surface in the blasted specimen.

3.3 Residual Stress

The blasted surface layer of a specimen was removed electrolytically by a given depth step by step and the change in strain on the opposite surface was measured in each removal with a strain gauge. Figure 6 shows the change in measured strains of a grit-blasted specimen and subsequently annealed specimens at different temperatures for 10.8 ks. The strains of the blasted specimen and the specimen annealed at 873 K become positive side and then remain unchanged, but the specimen annealed at 973 K exhibits no change in the measured strain. Thus, there is no residual stress in the specimen annealed at 973 K.

Figure 7 shows the residual stress distribution through thickness calculated from the inherent strain distribution curves, which are obtained from the measured strain curves. It is seen that a large compressive residual stress is distributed within the blasted specimens. The specimen reveals the maximum compressive residual stress of about 600 MPa at a depth of around 50 to $100 \mu\text{m}$ from the surface. It seems that the formation of martensite phase is related to the maximum stress in the blasted

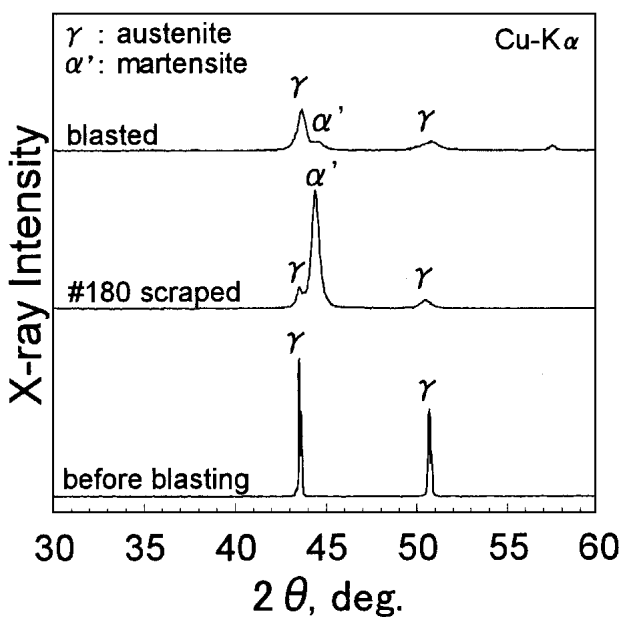


Fig. 4 XRD profiles of specimens

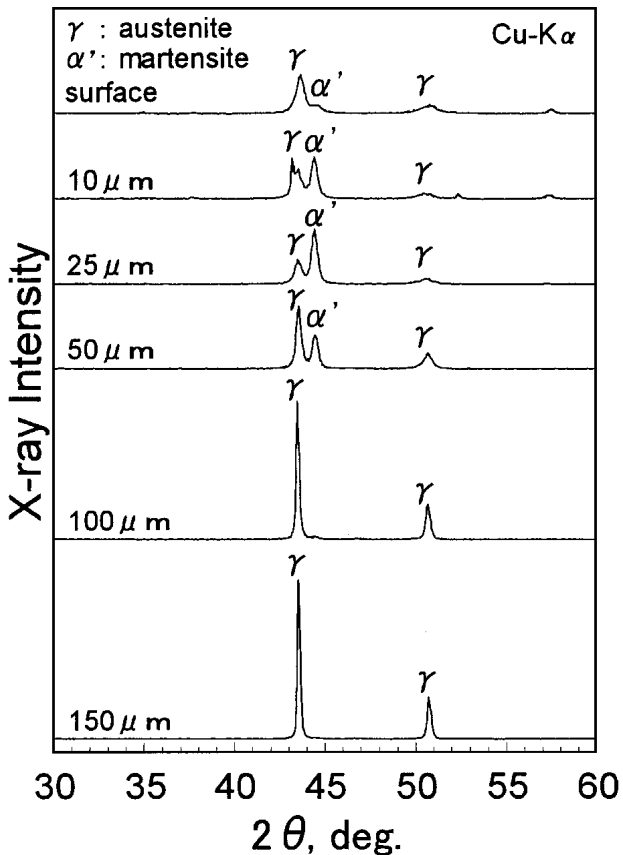


Fig. 5 XRD profiles of grit-blasted specimen at different distances from the surface

specimen. Annealing at 873 K released the residual stress in the area with the large stress of the blasted specimen and annealing at 973 K released the stress entirely.

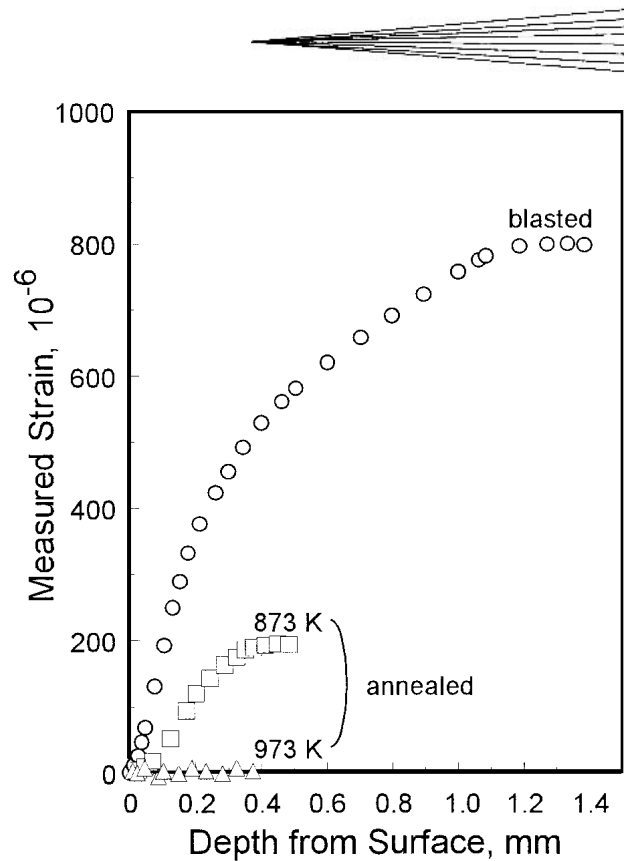


Fig. 6 Measured strain of grit-blasted specimen and annealed specimens as a function of depth from the surface

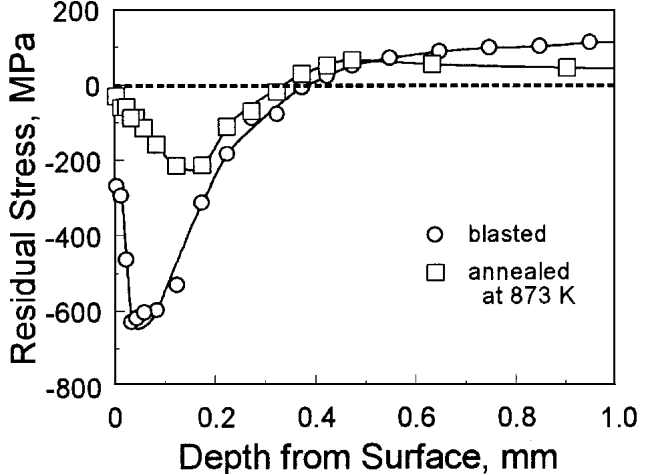


Fig. 7 Through-thickness residual stress distribution of grit-blasted specimen and annealed specimen as a function of depth from surface

3.4 Corrosion Resistance

Figure 8 shows anodic polarization curves of the grit-blasted and non-grit-blasted specimens in 1 N H_2SO_4 solution. The specimen solution treated at 1273 K in vacuum after grit blasting was measured to eliminate the influence of the martensite phase and the residual stress in the blasted specimen. All of the anodic polarization curves reveal an activation-passivation transition. The corrosion potentials of the blasted specimens are low com-

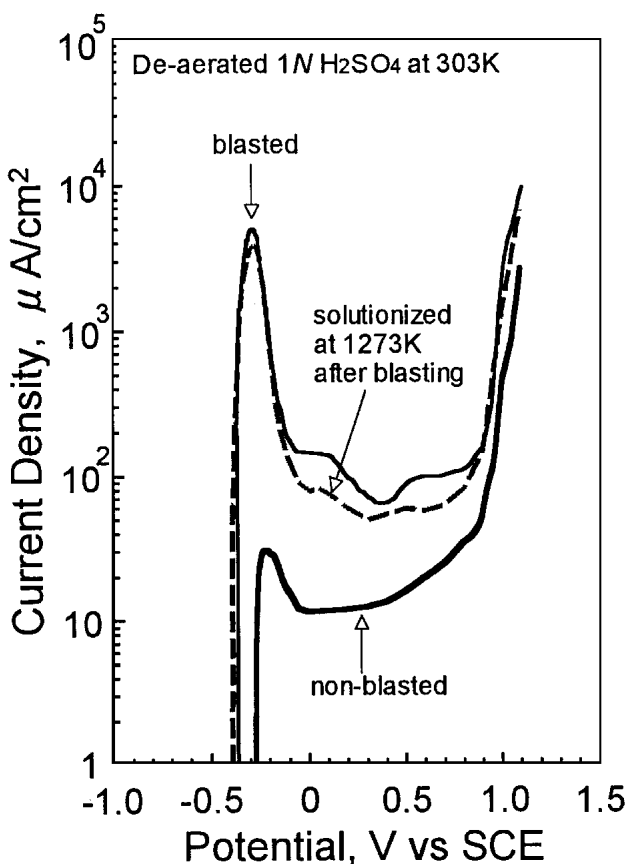


Fig. 8 Anodic polarization curves of specimens

pared with the non-blasted specimen and the passivation current density of the blasted specimen is much larger than that of the non-blasted specimen. Therefore, the blasting process deteriorates the corrosion resistance. However, the anodic polarization curve of the specimen subsequently solution treated at 1273 K in vacuum after blasting reveals almost the same curve as the blasted specimen. The deterioration of the corrosion resistance of the specimen is attributable to the roughened surface since the martensite phase disappears and the residual stress is released in the solution treated specimen.

Corrosion testing in 5% NaCl solution was carried out to evaluate the corrosion resistance of the roughened specimen. The specimens did not corrode when the specimens were dipped in the solution. Therefore, water-line attack due to the formation of an oxygen concentration cell was applied to evaluate the corrosion resistance. The specimens tilted 5° to the water line to be moved along the specimen surface by the natural evaporation of the solution (Fig. 9). Figure 10 shows the appearance of the blasted, non-blasted and abraded specimens after the corrosion test. It is shown that the blasted and subsequently solution treated specimens rust after the test (Fig. 10a,b), whereas the non-blasted and #180 abraded specimens did not rust though the volume fraction of martensite phase in #180 abraded specimen is large. From the results of the anodic polarization curves and the corrosion test, it is concluded that the deterioration of the corrosion resistance of the specimen by the blasting process is not caused by the formation of martensite phase and the generation

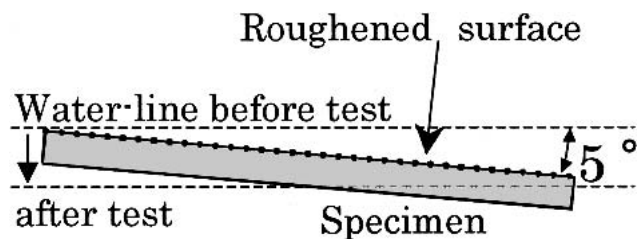


Fig. 9 Schematic illustration of corrosion test

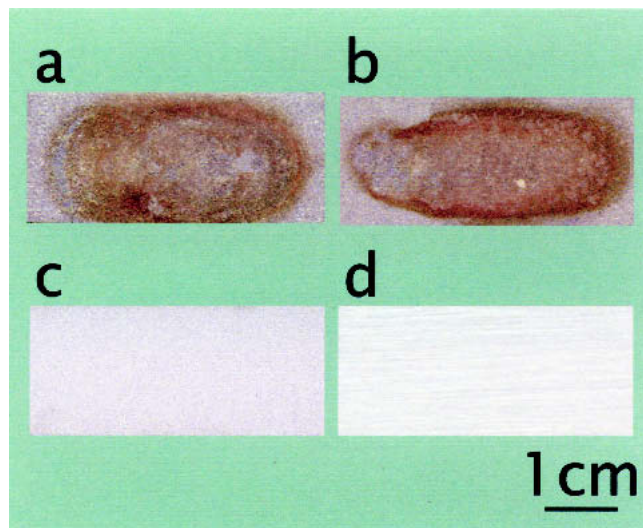


Fig. 10 Photos of specimen surface after immersion test: (a) grit-blasted specimen, (b) solution treated specimen after blasting, (c) non-blasted specimen, (d) #180 scraped specimen

of the residual stress but mainly by the change of surface morphology.

4. Conclusions

Surface roughness, structure, and residual stress distribution of the blasted SUS304 steel plate were investigated, and the effect of grit blasting on the corrosion resistance was examined with respect to the characterization. The results obtained are summarized as follows:

- The average roughness value of the grit-blasted surface is larger than the surface abraded with #180 abrasive paper.
- Martensite phase forms to the depth of 100 μm for grit-blasted specimen.
- Compressive residual stress is generated in the grit-blasted specimen and the maximum stress is at around 50 μm depth rather than the surface.
- The deterioration of the corrosion resistance of the blasted specimen is not attributable to the formation of martensite phase and the generation of the residual stress, but rather to the surface morphology of the specimen.

Acknowledgments

The authors wish to acknowledge the Center for Instrumental Analysis, Kyushu Institute of Technology for XRD analysis.

Also, the authors' thanks are due to Mrs. Zhensu Zeng of Kurashiki Boring Kiko. Co., Ltd. for salt spray tests.

References

1. Anon.: "Hot Rolled Stainless Steel Plates, Sheets and Strip," JIS G4304, 1999 (in Japanese).
2. Anon.: "Methods of Neutral Salt Spray Testing," JIS Z2371, 1994 (in Japanese).
3. K. Kon and T. Hisamatsu: "Stress Corrosion Cracking and (100) Faceting Dissolution of Pure Al-Cu Single Crystals," *Boshoku Gijutsu (Corrosion Engineering)*, 1977, 26, pp. 565-71 (in Japanese).
4. N. Ohtani: "Stress Corrosion Cracking," *Boshoku Gijutsu (Corrosion Engineering)*, 1977, 26, pp. 655-61 (in Japanese).
5. R.B. Mears and R.H. Brown: "Causes of Corrosion Currents," *Ind. Eng. Chem.* 1941, 33, pp. 1001-10.
6. K. Toshia and K. Lida: "Affected Layer Produced by Grit Blasting for Austenitic Stainless Steel," *Int. J. Japan Soc. Prec. Eng.*, 1995, 29(1), pp. 46-47.
7. J. Chen, T. Tersaki, T. Akiyama, and K. Kishitake: "Effect of Layer Removal Methods on Residual Stress Estimated by Inherent Strain Method," *Quart. J. Jpn. Weld. Soc.*, 1996, 14(4), pp. 762-67 (in Japanese).
8. Anon.: "Test Methods for Abrasion Resistance of Anodic Oxide Coatings on Aluminium and Aluminium Alloys-Part 1: Wheel Wear Test," JIS H8682-11999 (in Japanese).
9. T. Tersaki, S. Chen, T. Akiyama, and K. Kishitake: "Non-Destructive Method for Estimating Residual Stress Distribution in Component Due to Shot Peening," *Trans. Jpn. Soc. Mech. Eng.*, 1998, 64(618), pp. 353-59 (in Japanese).
10. R. Lagneborg: "The Martensite Transformation in 18% Cr-8% Ni Steels," *Acta Metall.*, 1964, 12, pp. 823-43.
11. F. Lecroisey and A. Pineau: "Martensitic Transformations Induced by Plastic Deformation in the Fe-Ni-Cr-C System," *Metall. Trans.*, 1972, 3, pp. 387-96.
12. T. Maekawa, N. Nakajima, and M. Kagawa: "Effect of Cold Working on Anodic Behavior of Stainless Steel in Sulfuric Acid Solution," *J. Jpn. Inst. Met.*, 1965, 29(3), pp. 248-52 (in Japanese).